Carbon Nanotube Yarn Electrodes for Enhanced Detection of Neurotransmitter Dynamics in Live Brain Tissue

Andreas C. Schmidt,[†] Xin Wang,[‡] Yuntian Zhu,[‡] and Leslie A. Sombers[†,*]

[†]Department of Chemistry and [‡]Department of Materials Science Engineering, North Carolina State University, Raleigh, North Carolina 27695, United States

ABSTRACT This work demonstrates the potential of nanoscale carbon electrode materials for improved detection of electroactive neurotransmitter dynamics in the brain. Individual multiwalled carbon nanotubes were synthesized *via* chemical vapor deposition, spun into yarns, and used in the fabrication of disk microelectrodes that were subsequently characterized using scanning electron and atomic force microscopies. The carbon nanotube yarn electrodes were coupled with fast-scan cyclic voltammetry and used to discriminately detect rapid neurotransmitter fluctuations in acute brain slices. The results demonstrate that the distinct structural and electronic properties of the nanotubes result in improved selectivity, sensitivity, and spatial resolution, as well as faster apparent electron transfer kinetics when compared to the conventional carbon-fiber microelectrodes typically used *in vivo*.

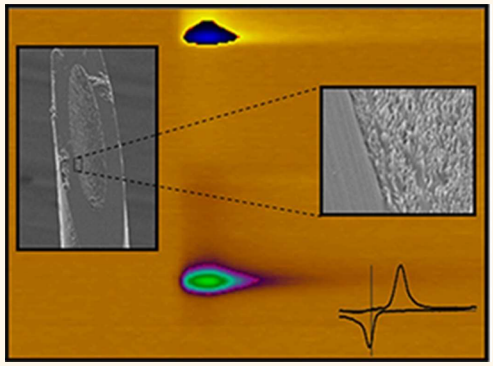

KEYWORDS: FSCV · carbon fiber · microelectrode · dopamine · voltammetry

Carbon-fiber microelectrodes (dimensions in the micrometer range) are a fundamental tool in the real-time electrochemical detection of neurotransmitters, including but not limited to dopamine,[1−7] adenosine,[8,9] hydrogen peroxide,[10] serotonin,[4,11−14] local pH changes,[5,15] and norepinephrine.[16,17] They are preferred for work in brain tissue due to their small size, which enables the detection of rapid chemical dynamics, minimizes tissue damage upon implementation, and provides excellent spatial resolution for sampling from discrete neural circuits.[18] Compared to larger electrodes, microelectrodes offer highly increased diffusional flux to the electrode surface, decreased ohmic drop, and faster response times that enable high speed measurements.[19] Furthermore, carbon-fiber microelectrodes are biologically compatible, have a wide potential window and renewable surface,[20] and are easily coupled with fast-scan cyclic voltammetry (FSCV).[21,22] FSCV provides the temporal resolution required for measuring neurotransmitter release on a subsecond time scale and enables qualitative identification of an analyte through a distinctive cyclic voltammogram. Thus the combination of FSCV with carbon-fiber microelectrodes is a powerful tool for making rapid measurements in complex environments such as the brain.

Since Wightman[23,24] and others[25−27] initially reported the fabrication and characterization of ultramicroelectrodes in the early 1980s, a significant amount of research across many laboratories has focused on enhancing the detection capabilities of the carbon-fiber electrode material by modifying the surface in different ways. Nafion is a commonly used perfluorinated cation exchange polymer that is deposited onto the carbon surface to improve sensitivity for cationic species, such as dopamine.[28−31] However, electrode coatings necessarily slow the electrode time response by hindering analyte diffusion to the electrode surface. The sensitivity of carbon-fiber electrodes can also be increased by electrochemical pretreatment[2,32,33] and surface cleaning.[34] Finally, carbon nanotubes (CNTs) can enhance

* Address correspondence to leslie_sombers@ncsu.edu.

Received for review June 6, 2013 and accepted August 13, 2013.

Published online August 13, 2013
10.1021/nn402857u

sensitivity when deposited onto the carbon surface.[9,35,36] The demonstrated benefit of enhanced mass transport to very small electrodes underlies a broad interest in the use of CNTs, which offer a high aspect ratio, for electrochemical analysis in biological systems. Indeed, interest in CNT technology has significantly grown over the past two decades. CNTs provide high tensile strength and stiffness, as well as good thermal and electrical conductivity.[37] Furthermore, CNTs can be spun into continuous fibers to form a yarn.[38−40] The yarn diameter is dependent on the diameter of the individual nanotubes, as well as the twisting angle used in spinning. Thus, the yarns are customizable and can be tailored with diameters and lengths suitable for use in electrodes dedicated to a variety of applications. Electrochemical sensors spun from CNTs were first reported in 2003,[41] and glucose measurements using dry-spun CNT-yarn electrodes modified with glucose oxidase have been reported by Zhu *et al.*[42,43] CNT fibers have been used to detect dopamine using differential pulse voltammetry[44] and amperometry,[45] have been incorporated into electrode arrays,[46] and have also been suggested to be a superior deep brain stimulating electrode when compared to other electrode materials,[47] hinting at their *in vivo* potential.

In order to take advantage of the unique properties of CNTs and the mass transfer benefits of working at the nanoscale, we have utilized a multiwalled carbon nanotube (MWNT) yarn as the sole sensing substrate in elliptical disk microelectrodes. We have quantitatively characterized the performance of the CNT yarn disk-shaped (CNTy-D) electrodes when coupled with FSCV and have systematically compared them to conventional carbon-fiber microelectrodes for the detection of neurotransmitters. The MWNT yarn used herein was composed of individual MWNTs (~40−50 nm diameter) spun into a continuous fiber with a diameter of 30 μm and a twist angle of 20°. The CNTy-D electrodes had a sensing surface composed of highly curved carbon nanotubes that was physically characterized using scanning electron microscopy (SEM) and atomic force microscopy (AFM). The electrodes were electrochemically characterized using FSCV. They exhibited lower background currents, improved current density, and faster apparent electron transfer kinetics when compared to more conventional carbon-fiber electrodes, resulting in improved sensitivity and selectivity. Finally, these novel CNTy-D electrodes were used to discriminately detect dopamine in acute brain slices, demonstrating their potential as an attractive tool to advance the detection of dynamic chemical fluctuations in discrete biological locations.

RESULTS AND DISCUSSION

Research in the area of microelectrodes became very active in the late 1970s, coincident with advances in the field of microelectronics and the advent of microstructural materials.[19] The unique advantages of small electrodes opened up many areas of study that were inaccessible with electrodes of larger size, including detection of the kinetics of electroactive neurotransmitter molecules in the brain.[48,49] Today, some 35 years later, electrochemistry is a benchmark tool in neuroscience. Thus, it is no surprise that there is a broad interest in exploiting the unique properties of carbon-based nanomaterials for electrochemical analyses in biological systems. Further miniaturization to the nanoscale promises to enhance the very characteristics that made microelectrodes so transformative, enabling high speed measurements in discrete spatial locations. Herein, we have demonstrated the potential of yarns spun from CNTs for enhanced neurotransmitter detection in live tissue.

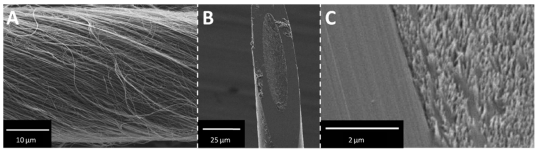

Figure 1. Scanning electron micrographs of a CNTy-D electrode. (A) Spun MWNTs form a continuous yarn. (B) A single CNTy-D electrode. (C) Detailed image of CNT surface and glass seal of the CNTy-D electrode.

Physical Characterization of Carbon Nanotube Yarn as an Electrode Substrate. A 1 m length of carbon nanotube yarn was spun from a forest of 40−50 nm diameter individual ultralong multiwalled carbon nanotubes. The yarn, shown in Figure 1A, was approximately 30 μm in diameter with a twist angle of 20°. It was then used to fabricate microdisk electrodes, polished at 30° to form an elliptical sensing surface (Figure 1B). The minor diameter of the sensing surface is 17.3 ± 0.4 μm (n = 5), because the yarn tightens as it is pulled in the micropipet puller. On the sensing surface, the ends of the nanotubes are distinguishable from the glass seal and can be recognized in the higher magnification scanning electron micrograph shown in Figure 1C.

Throughout this work, CNTy-D electrodes (geometric sensing area = 8.08 (±0.86) × 10^{-6} cm^2, n = 5) are compared to conventional cylindrical carbon-fiber microelectrodes (7 μm diameter × 100 μm long, geometric sensing area of ~2.24 × 10^{-5} cm^2), as cylindrical carbon-fiber microelectrodes are typically used for dopamine detection *in vivo*.[1,3−7,50] Disk electrodes made from conventional carbon fibers do not offer sufficient sensitivity for work in live tissue. Because voltammetric current is proportional to the electrode surface area, atomic force microscopy (AFM) was used to estimate the roughness of the CNTy-D sensing surface, compared to that of conventional carbon-fiber microdisk electrodes. Quantitative analysis of these data indicated that the root mean squared (rms) roughness value inherent to the sensing surface of a standard

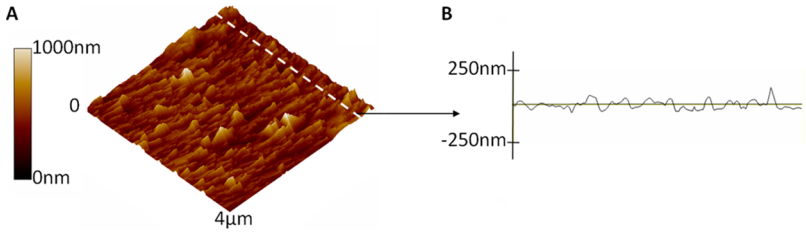

Figure 2. (A) Representative three-dimensional AFM image of the CNTy-D electrode sensing surface, and (B) the associated line plot from this sample.

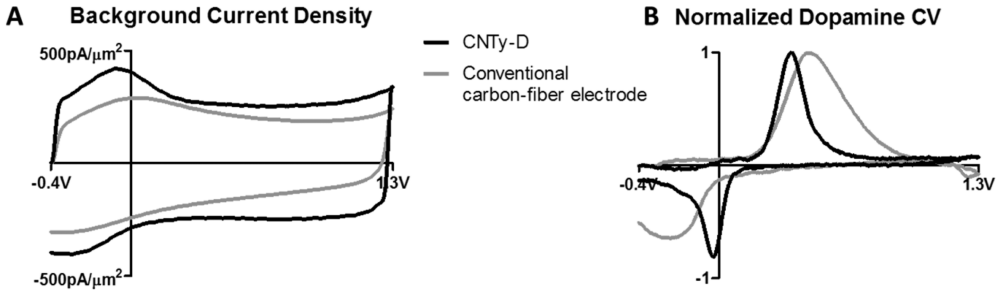

Figure 3. Fast-scan cyclic voltammetry at a conventional carbon-fiber microelectrode and a CNTy-D electrode. (A) Representative cyclic voltammograms depicting non-faradaic background charging current. The charging current densities recorded at the carbon-fiber microelectrode (gray) and the CNTy-D electrode (black) are similar in magnitude. (B) Representative normalized voltammograms for 1 μM dopamine collected at both electrode subtypes. The voltammogram collected using the CNTy-D electrode clearly exhibits a decreased peak-to-peak separation.

TABLE 1. Analysis of Anodic and Cathodic Peak Currents, Redox Potentials, and Peak-to-Peak Separation for the Detection of 1 μM Dopamine[a]

	i_{pa} (nA)	i_{pc} (nA)	i_{pc}/i_{pa}[b]	E_{pa} (V)[b]	E_{pc} (V)[b]	ΔE_p (V)[b]
CNTy-D	22.67 ± 2.34	20.17 ± 2.45	0.89 ± 0.04	0.34 ± 0.02	−0.06 ± 0.02	0.40 ± 0.01
conventional	19.78 ± 2.82	13.14 ± 2.53	0.66 ± 0.03	0.47 ± 0.01	−0.17 ± 0.01	0.64 ± 0.02

[a] $n = 6$, data are mean ± SEM. Significant differences between CNTy-D and conventional carbon-fiber microelectrodes were determined by unpaired t test. [b] $p < 0.001$.

carbon-fiber disk electrode was 13.8 (±0.8) nm, whereas the roughness of the CNTy-D sensing surface was significantly greater at 58.1 (±6.7) nm ($p < 0.001$, $n = 4$). A representative AFM image of the sensing surface of the CNTy-D electrode is shown in Figure 2. An AFM image of the sensing surface of a standard carbon-fiber disk electrode can be seen in reference 2.

Electrochemical Characterization of Carbon Nanotube Yarn Using Fast-Scan Cyclic Voltammetry. In FSCV, application of the electrochemical waveform generates a large, non-faradaic background current, even in the absence of analyte. This current is largely due to charging of the double layer at the electrode surface.[53] It is dependent on electrode capacitance, which is proportional to electrode area. Figure 3A compares the background current density (current divided by geometric sensing area) between the CNTy-D electrodes and cylindrical carbon-fiber electrodes. The background current density is comparable between the two electrode types (Figure 3A), but there are subtle differences in the shape of these voltammograms. These differences are more readily apparent when investigating the normalized background-subtracted cyclic voltammograms for 1 μM dopamine (Figure 3B). The oxidative and reductive peaks for dopamine occur at reduced overpotentials when using the CNTy-D electrodes. Furthermore, the cathodic/anodic peak current ratio is significantly greater for CNTy-D electrodes than for conventional carbon-fiber electrodes ($p < 0.001$, $n = 6$). These results are summarized in Table 1. They reflect both faster (apparent) electron transfer kinetics at the CNTy-D electrode substrate, as well as a different mass transport profile at the surface of this sensor.

Figure 4A compares simulated voltammograms for 1 μM dopamine detection at cylindrical and disk microelectrodes. The simulation utilizes a finite difference model[51,52] and a diffusion coefficient of 7×10^{-6} cm^2/s. The rate constant for electron transfer (k) was chosen to be 3×10^{-6} cm/s, to fit the experimental data. A greater cathodic/anodic peak current ratio is evident in the data simulated for the disk microelectrode. Figure 4B overlays voltammograms collected at the CNTy-D and conventional carbon-fiber microelectrodes. The peak oxidation potential predicted by the simulation (~0.46 V) correlates with the peak oxidation potential evident in the voltammograms collected using the conventional carbon-fiber microelectrodes (dashed line). However, voltammograms collected using

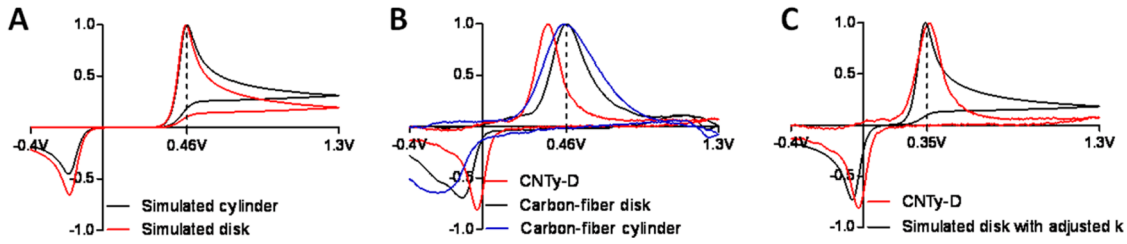

Figure 4. Voltammograms collected using the CNTy-D microelectrodes exhibit well-defined oxidative and reductive peaks at significantly reduced overpotentials, as well as an enhanced cathodic/anodic peak current ratio. (A) Simulated and (B) experimental voltammograms generated at cylindrical and disk microelectrodes in response to 1 μM dopamine. Simulations were performed using $D = 7 \times 10^{-6}$ cm^2/s. (C) Increasing k (cm/s) by 2 orders of magnitude results in a simulated voltammogram that closely resembles the electrochemical response observed on CNTy-D electrodes.

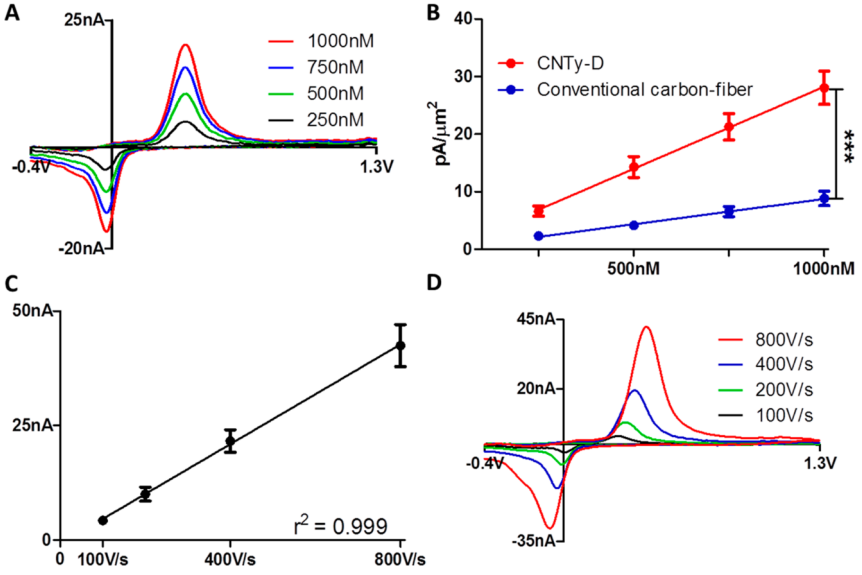

Figure 5. Dopamine voltammetry on carbon nanotube yarn electrodes. (A) Representative voltammograms for physiological concentrations. (B) Calibration curve. The CNTy-D electrodes (red) are significantly more sensitive than conventional carbon-fiber microelectrodes (blue, $p < 0.001$, Student's t test, $n = 6$). (C) Anodic current increases linearly with scan rate when detecting 1 μM dopamine using CNTy-D electrodes. (D) Voltammograms collected at scan rates ranging from 100 to 800 V/s. Faster scan rates increase sensitivity and ΔE_p.

the CNTy-D microelectrodes exhibit oxidative and reductive peaks at significantly reduced overpotentials and a diminished peak width as compared to conventional carbon-fiber electrodes. This is in agreement with previous research that has suggested that modifying a carbon-fiber with CNTs can provide superior apparent electron transfer kinetics.[11,54,55] Indeed, the voltammograms collected using the CNTy-D electrodes could be forced to match the voltammograms simulated for disk-shaped microelectrodes by increasing k by 2 orders of magnitude (Figure 4C). However in electrochemical monitoring, mass transport to the sensor surface also plays a large role in determining the electrochemical response. A previous work has shown that voltammograms collected at glassy carbon electrodes modified with MWNTs were effectively simulated by a model incorporating a 'thin layer' mass transport regime; a change in electrode kinetics was not required.[56] Those voltammograms exhibited anodic peaks that were shifted to more negative potentials, even approaching their formal potential values when the distance between individual nanotubes on the carbon surface was minimized. However, the detection of dopamine is adsorption-controlled, and a distinction between thin-layer and adsorption effects is not easily made.

A series of representative voltammograms collected for the detection of dopamine using the CNTy-D electrodes is shown in Figure 5A. A full data set was used to construct a linear calibration curve for both the CNTy-D and standard cylindrical carbon-fiber microelectrodes, where current density was plotted *versus* analyte concentration (Figure 5B). A calibration curve that does not account for electrode area (plotting current *versus* analyte concentration) is presented as Supplementary Figure S1. The CNTy-D electrodes are significantly more sensitive than the conventional carbon-fiber microelectrodes ($p < 0.001$, $n = 6$), as a result of the enhanced mass transport to this modified surface. They also exhibit a significantly lower theoretical limit of detection (defined as three times the standard deviation of the noise) when compared to

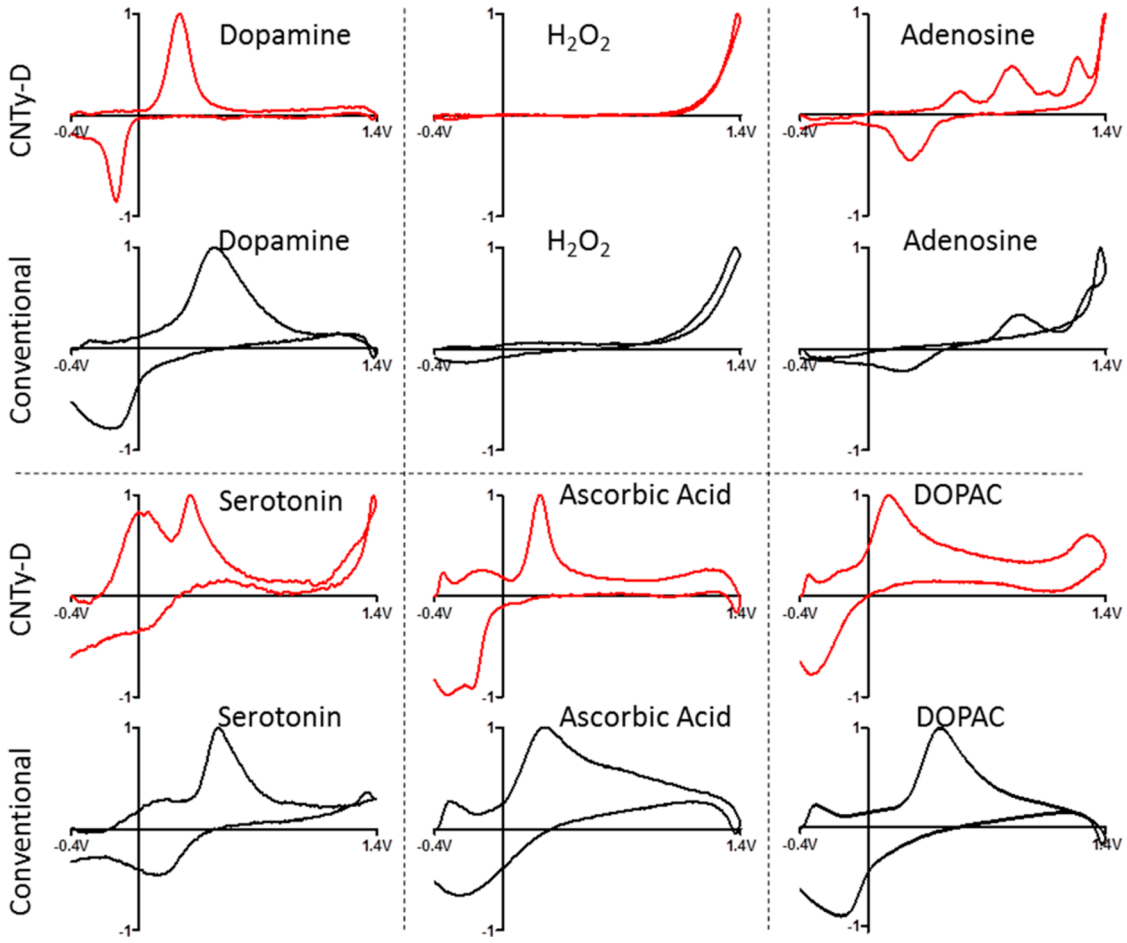

Figure 6. Voltammograms for several analytes commonly encountered in brain tissue. Normalized data collected using CNTy-D electrodes are shown in red, and those collected using conventional carbon-fiber electrodes are shown in black. Potential was scanned from −0.4 to +1.4 V and back at 400 V/s and applied at 10 Hz to allow for the detection of many analytes.

conventional carbon-fiber electrodes (13.4 ± 1.7 nM and 20.8 ± 1.3 nM, respectively, $p < 0.01$, $n = 9$). This is due to the low noise inherent to the CNTy-D electrodes. The detection of dopamine at carbon-fiber electrodes is adsorption-controlled, and thus the measured current increases linearly with scan rate.[57] This relationship also holds at the CNTy-D electrodes (Figure 5C). Using faster scan rates necessarily increases the peak-to-peak separation; however, even at 800 V/s the peaks were completely resolved in the potential window. This demonstrates that faster scan rates, even beyond those used here, can be exploited with this nanoscale electrode material to further increase sensitivity and temporal resolution.

Carbon Nanotube Yarn Facilitates Voltammetric Discrimination between Species. A major strength of voltammetry is its ability to resolve multiple analytes in a complex mixture. This is done by evaluating voltammetric peak shape and position. To distinguish between chemical species that are involved in diffusion-controlled, one-electron electrolysis processes, the $E^{o'}$s must differ by at least 0.118 V.[58] Thus, sharp and well-defined peaks are a significant advantage when resolving multiple compounds, such as in the complex environment of the brain. Voltammograms for several analytes commonly encountered in live brain tissue were collected using a broadly applicable electrochemical waveform at CNTy-D and conventional cylinder carbon-fiber microelectrodes. The normalized voltammograms are compared in Figure 6. In all cases, the voltammograms collected using the CNT yarn (red) exhibit sharper peaks and faster apparent electron transfer kinetics when compared to the conventional carbon-fiber microelectrodes (black), as well as enhanced cathodic/anodic current ratios. However, it must be noted that the optimized waveform for serotonin detection[14] is considerably different from the one applied here. Interestingly, when using the CNTy-D electrode an extra peak is evident in the voltammogram for adenosine (~530 mV) that has not been previously reported when using a similar voltammetric waveform.[9] This peak could aid in distinguishing adenosine from other analytes that have electrochemical features evident near the switching potential, such as H_2O_2,[10,59] histamine,[60−62] and shifts in pH.[15] It is likely a product of adenosine polymerization onto the

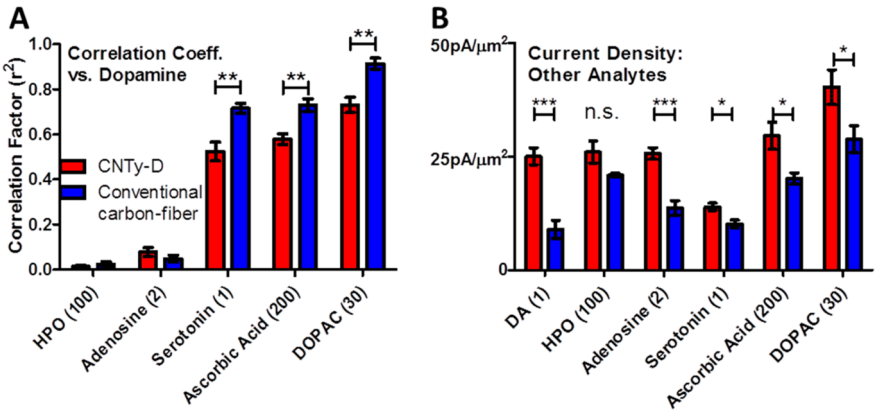

Figure 7. Carbon nanotube yarn electrodes demonstrate enhanced selectivity and sensitivity for multiple analytes. (A) The square of the correlation coefficient (r^2) for correlations between the voltammogram of each analyte and the voltammogram for dopamine collected using CNTy-D electrodes (red) and conventional carbon-fiber microelectrodes (blue). (B) Current density is significantly enhanced for dopamine, adenosine, serotonin, ascorbic acid, and DOPAC detection using CNTy-D electrodes. The numbers in parentheses on the *x*-axis indicate the concentration used in μM. The data is mean $\pm$ SEM, compared using Student's *t* test, $n = 5$; *$p < 0.05$, **$p < 0.01$, ***$p < 0.001$, respectively.

electrode surface, as it develops on a slower time scale (Supplementary Figure S2). Finally, the voltammogram for norepinephrine is indistinguishable from that of dopamine,[16] and the CNTy-D electrodes did not improve this issue (data not shown).

To quantify the extent to which the carbon nanotube yarn facilitates voltammetric discrimination between species, a correlation coefficient (*r*) was calculated for a comparison of the voltammogram for each analyte to that of dopamine. A squared correlation factor of 1.00 indicates an exact match; therefore a lower correlation factor indicates improved discrimination between the analytes. The results show that CNTy-D electrodes are significantly better able to distinguish ascorbic acid, serotonin, and DOPAC from dopamine, when compared to conventional carbon-fiber microelectrodes (Figure 7A). Adenosine and H_2O_2 have low correlations to dopamine on both electrode materials, and thus no significant improvement was observed. These data can also be used to assess sensitivity. The current density for all of the analytes, with the exception of H_2O_2, is significantly greater on CNTy-D electrodes than on the conventional carbon-fiber electrodes (Figure 7B). These results demonstrate not only that the CNTy-D electrodes are more adept at distinguishing dopamine from other analytes but also that dopamine detection is most significantly enhanced (180% signal enhancement). This is likely due to the development of additional oxygen-containing functional groups on the abundant edge plane sites inherent to carbon nanotubes.[63] This would create a favorable electrostatic interaction between positively charged dopamine and the electrode surface, while also creating an electrostatic repulsion for ascorbic acid and DOPAC, which are negatively charged at physiological pH. Adenosine and H_2O_2 are neutral at physiological pH. Serotonin is positively charged at physiological pH; however, it is also known to foul the electrode surface when applying the waveform used here.[13] Such fouling could be enhanced at the CNTy-D electrode, due to the large surface area and the oxygen functionalities inherent to the exposed nanotube ends. This would diminish signal enhancement. However, a recent report noted that carbon nanotube fiber microelectrodes show a higher resistance to dopamine fouling when compared to traditional carbon-fiber microelectrodes.[45]

Voltammetric Detection of Dopamine in Live Brain Tissue. To directly demonstrate that CNTy-D electrodes provide an attractive alternative to standard cylindrical carbon-fiber microelectrodes for work in brain tissue, single CNTy-D microelectrodes were inserted at least 100 μm into a section of a rat brain slice (400 μm overall slice thickness) that encompassed the striatum, a region with nerve terminals containing the neurotransmitter dopamine. A bipolar stimulating electrode was placed in the vicinity of the working electrode, and dopamine release was electrically evoked. Representative voltammetric data are presented in Figure 8. Figure 8B shows a representative data set of 300 background-subtracted cyclic voltammograms. The applied potential (V) is the ordinate, the time (s) is the abscissa, and current (nA) is depicted in false color.[65] Plotting the data in this way enables visualization of current collected across the entire potential range and facile identification of interfering species and noise. No current is detected until the onset of the electrical stimulation (arrow), and the current is selectively associated with the oxidation and reduction of dopamine. Figure 8A presents the concentration *versus* time trace created by extracting the current at the peak oxidation potential for dopamine (dashed horizontal line) and converting it to concentration upon electrode calibration. A single cyclic voltammogram extracted from the data (dashed vertical line) is presented in the inset in Figure 8A. These data demonstrate that the CNTy-D microelectrodes are well suited for work in

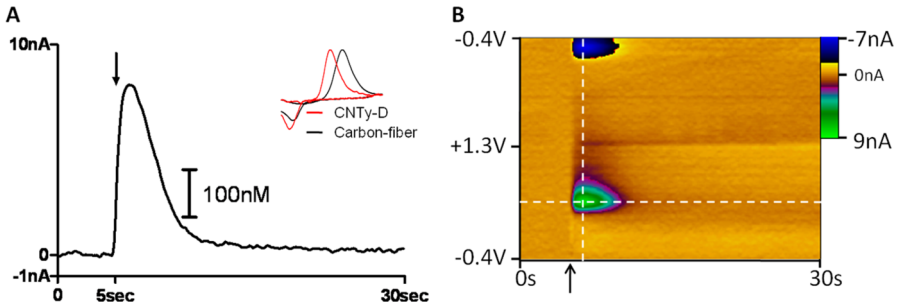

Figure 8. Endogenous dopamine detection using disk-shaped carbon nanotube yarn electrodes in living brain tissue. (A) Representative current *versus* time trace collected at the peak oxidation potential for dopamine with concentration determined by electrode calibration. Electrical stimulation occurred at the time indicated by the arrow. Inset: Normalized representative voltammograms corresponding to dopamine on CNTy-D (red) and conventional carbon-fiber (black) electrodes. (B) Three-dimensional colorplot of raw data collected in striatal tissue using a CNTy-D electrode. The ordinate is the applied potential, the abscissa is time (s), and the current (nA) is depicted in false color.

brain tissue, as they retain a low noise profile at all potentials and serve to readily quantify dopamine fluctuations in the striatum. They also offer an electrode geometry that enables sensing from discrete neural circuits.

CONCLUSION

We have shown that microelectrodes constructed from a carbon nanotube yarn provide an attractive alternative to conventional carbon-fiber microelectrodes offering several advantages. These electrodes exhibit faster apparent electron transfer kinetics that are manifested as sharper voltammetric peaks. As a consequence, qualitative identification of analytes is enhanced. Additionally, we have shown that the CNTy-D electrodes exhibit an enhanced sensitivity to many analytes commonly encountered in brain tissue. This work demonstrates that crafting electrodes made purely of carbon nanotubes is a viable and promising approach to improve the spatial, temporal, and electrochemical resolution of *in vivo* electrochemistry, even in the absence of a conventional base electrode substrate for detection within living tissue. It lays the foundation for a new generation of *in vivo* sensors; however, it is only a preliminary exploration of the potential offered by this new technology. The properties of the carbon nanotube yarns are dependent on the nanotubes used to create them, as well as the twist angle used in spinning. Thus, the material is highly customizable and can be tailored to the kinetic and spatial constraints associated with a given electrochemical experiment.

METHODS

Chemicals. All chemicals were purchased from Sigma-Aldrich (St. Louis, MO) and used as received, unless otherwise specified. Electrochemical experiments were carried out in phosphate buffered saline (0.1 M PBS) at physiological pH 7.4. Brain slice experiments used artificial cerebral spinal fluid (aCSF) saturated with 95% O_2 and 5% CO_2, at physiological pH 7.4. aCSF consisted of 124 mM NaCl, 26 mM $NaHCO_3$, 3.7 mM KCl, 2.4 mM $CaCl_2$, 1.3 mM $MgCl_2$, 1.3 mM NaH_2PO_4, and 10 mM glucose. All aqueous solutions were made from double deionized water >18 MΩ cm (Millipore, Billerica, MA).

Carbon Nanotube Yarn Fabrication. The vertically aligned multiwalled carbon nanotube (MWCNT) arrays were grown on quartz substrates by the "chloride mediated chemical vapor deposition (CVD)" method.[66] The as-synthesized MWCNTs had a height of 1.1 mm, an outer diameter of ~40−50 nm, and approximately 40 walls. The array height was measured using a calibrated scale bar in an optical microscope (30×). The diameter of the MWCNTs was measured using ImageJ software, based on the transmission electron microscopy (TEM) images acquired by a JEOL 2000FX TEM operated at 200 kV. CNT ribbons maintained at 4 mm width were pulled out from the array by hand using tweezers and then attached to a spindle using a piece of double-sided tape. CNT yarns were formed by simultaneous drawing and rotating of the spindle. The twist angle and yarn diameter were measured by a JEOL 6400 scanning electron microscope (SEM) and were maintained at ~20° and ~30 μm, respectively.

Electrode Fabrication. All electrochemical experiments were carried out with cylindrical carbon-fiber microelectrodes created using T-650/35 PAN based carbon fibers (T-650), microdisk electrodes created using P-55 PITCH based carbon fibers (P-55) (both Cytec Industries, West Patterson, NJ), or disk microelectrodes created using the carbon nanotube yarn (CNTy-D electrodes). The cylinder microelectrodes were fabricated as described previously.[50] Briefly, a single 7 μm diameter fiber was aspirated into a single borosilicate glass capillary (1.0 mm × 0.5 mm, A-M Systems, Carlsburg, WA). Using a micropipet puller (Narishige, Tokyo, Japan) the glass was tapered to form sealed microelectrodes that were cut to a length of 100 μm of exposed carbon. Disk-shaped microelectrodes were fabricated in a similar fashion, except that pulled microelectrodes were cut at the glass seal, then dipped in epoxy for 30 s, and oven-dried. Finally, the electrodes were polished at a 30° angle into an elliptical disk (Figure 1B).

Geometric sensing areas were calculated on the basis of electrode diameter. The diameter of disk electrodes was estimated by averaging the long and short axes of the elliptical sensing area evident in the SEMs. For CNTy-D electrodes, this area was calculated to be 8.08 (±0.86) × 10^{-6} cm^2 (n = 5). The true surface area is likely to be larger due to the roughness inherent to the surface.

To establish an electrical connection with the carbon, the glass capillary was backfilled with ionic solution (4 M potassium acetate, 150 mM KCl), and a lead was inserted. All measurements were recorded against a Ag/AgCl reference electrode (World Precision Instruments, Inc., Sarasota, FL).

Surface Analysis. AFM of the electrode surface was done with a Veeco D3000 microscope (Plainview, NY) using tips from Nanosensors (PPP-HCH, Neuchatel, Switzerland) with a nominal resonance of 280 kHz.

Flow Injection. All data, with the exception of brain slice experiments, were collected in a custom-built flow injection apparatus housed within a Faraday cage. A syringe pump (New Era Pump Systems, Inc., Wantagh, NY) supplied a continuous buffer flow of 1 mL/min across both the working and reference electrode. The working electrode was lowered into the electrochemical cell *via* a micromanipulator (World Precision Instruments, Inc., Sarasota, FL). Two-second bolus injections of analyte were accomplished using a six-port HPLC valve and air actuator controlled by a digital valve interface (Valco Instruments Co., Inc., Houston, TX).

Electrochemical Waveforms and Data Acquisition. A triangular waveform was used for analyte detection. The applied potential ranged from −0.4 to +1.3 V and back to −0.4 V unless otherwise specified. It was scanned at a rate of 400 V/s and applied at a frequency of 10 Hz. The CNTy-D electrodes were electrochemically pretreated for 1 min using a waveform ranging from −0.5 to 1.6 V, applied at 10 Hz. The conventional carbon-fiber electrodes were not pretreated in this way as some became unusable after the treatment. The waveforms were output using a custom-built instrument for potential application to the electrochemical cell and current transduction (University of North Carolina at Chapel Hill, Department of Chemistry, Electronics Facility). TH-1 software (ESA, Chelmsford, MA) was used for waveform output with a DAC/ADC card (NI 6251 M). A second card (NI 6711) was used for synchronization of the electrochemical experiment with the flow injection system. Signal processing (background subtraction and signal averaging) was software-controlled.

Brain Slice Preparation. Male Sprague-Dawley rats (250−300 g, Charles River Laboratories, Raleigh, NC) were decapitated after being deeply anesthetized with urethane (1.5 g/kg, ip). The brain was rapidly removed, mounted, and placed in cold aCSF. Coronal slices with a thickness of 400 μm containing the striatum were obtained with a vibratome (World Precision Instruments, Sarasota, FL). The slices were allowed to rest in the buffer for at least 1 h before the start of an experiment. Brain slices were subsequently placed in a recording chamber (Warner Instruments, Hamden, CT) and superfused with aCSF buffer maintained at 34 °C for at least 1 h. The working electrode and bipolar stimulating electrode placements were made with the aid of a microscope (Nikon Instruments, Inc., Melville, NY), and the microelectrodes were positioned about 100 μm below the surface of the slice. Electrical stimulation of nerve terminals consisted of five 500 μA pulses at 60 Hz using a pulse width of 4 ms. Animal care and use was in complete accordance with institutional guidelines and IACUC.

Data Analysis and Statistics. All data presented are shown as the mean ± standard error of the mean (SEM). Unpaired *t* tests were used to determine the significance of means between two groups. Statistical and graphical analyses were carried out using GraphPad Prism 5 (GraphPad Software, Inc., La Jolla, CA). Digital simulation was performed using DigiSim Simulation Software for Voltammetry (BASi, West Lafayette, IN).

Conflict of Interest: The authors declare no competing financial interest.

Acknowledgment. We thank the Chemistry Department (North Carolina State University) for funding this work, Chuck Mooney (Analytical Instrumentation Facility, North Carolina State University) for assistance with imaging, and Greg McCarty (The Joint Department of Biomedical Engineering, North Carolina State University/University of North Carolina) for helpful discussion and careful review of the manuscript.

Supporting Information Available: Supplemental figures. This material is available free of charge *via* the Internet at http://pubs.acs.org.

REFERENCES AND NOTES

1. van Zessen, R.; Phillips, J. L.; Budygin, E. A.; Stuber, G. D. Activation of VTA GABA Neurons Disrupts Reward Consumption. *Neuron* **2012**, *73*, 1184–1194.
2. Roberts, J. G.; Moody, B. P.; McCarty, G. S.; Sombers, L. A. Specific Oxygen-Containing Functional Groups on the Carbon Surface Underlie an Enhanced Sensitivity to Dopamine at Electrochemically Pretreated Carbon Fiber Microelectrodes. *Langmuir* **2010**, *26*, 9116–9122.
3. Lemos, J. C.; Wanat, M. J.; Smith, J. S.; Reyes, B. A. S.; Hollon, N. G.; Van Bockstaele, E. J.; Chavkin, C.; Phillips, P. E. M. Severe Stress Switches CRF Action in the Nucleus Accumbens from Appetitive to Aversive. *Nature* **2012**, *490*, 402–406.
4. John, C. E.; Budygin, E. A.; Mateo, Y.; Jones, S. R. Neurochemical Characterization of the Release and Uptake of Dopamine in Ventral Tegmental Area and Serotonin in Substantia Nigra of the Mouse. *J. Neurochem.* **2006**, *96*, 267–282.
5. Ariansen, J. L.; Heien, M.; Hermans, A.; Phillips, P. E. M.; Hernadi, I.; Bermudez, M. A.; Schultz, W.; Wightman, M. Monitoring Extracellular pH, Oxygen, and Dopamine During Reward Delivery in the Striatum of Primates. *Front. Behav. Neurosci.* **2012**, *6* (36), 1−10.
6. Sombers, L. A.; Beyene, M.; Carelli, R. M.; Wightman, R. M. Synaptic Overflow of Dopamine in the Nucleus Accumbens Arises from Neuronal Activity in the Ventral Tegmental Area. *J. Neurosci.* **2009**, *29*, 1735–1742.
7. Roitman, M. F.; Wheeler, R. A.; Wightman, R. M.; Carelli, R. M. Real-Time Chemical Responses in the Nucleus Accumbens Differentiate Rewarding and Aversive Stimuli. *Nat. Neurosci.* **2008**, *11*, 1376–1377.
8. Swamy, B. E. K.; Venton, B. J. Subsecond Detection of Physiological Adenosine Concentrations Using Fast-Scan Cyclic Voltammetry. *Anal. Chem.* **2007**, *79*, 744–750.
9. Ross, A. E.; Venton, B. J. Nafion-Cnt Coated Carbon-Fiber Microelectrodes for Enhanced Detection of Adenosine. *Analyst* **2012**, *137*, 3045–3051.
10. Sanford, A. L.; Morton, S. W.; Whitehouse, K. L.; Oara, H. M.; Lugo-Morales, L. Z.; Roberts, J. G.; Sombers, L. A. Voltammetric Detection of Hydrogen Peroxide at Carbon Fiber Microelectrodes. *Anal. Chem.* **2010**, *82*, 5205–5210.
11. Swamy, B. E. K.; Venton, B. J. Carbon Nanotube-Modified Microelectrodes for Simultaneous Detection of Dopamine and Serotonin *in Vivo*. *Analyst* **2007**, *132*, 876–884.
12. Borue, X.; Cooper, S.; Hirsh, J.; Condron, B.; Venton, B. J. Quantitative Evaluation of Serotonin Release and Clearance in Drosophila. *J. Neurosci. Methods* **2009**, *179*, 300–308.
13. Jackson, B. P.; Dietz, S. M.; Wightman, R. M. Fast-Scan Cyclic Voltammetry of 5-Hydroxytryptamine. *Anal. Chem.* **1995**, *67*, 1115–1120.
14. Hashemi, P.; Dankoski, E. C.; Petrovic, J.; Keithley, R. B.; Wightman, R. M. Voltammetric Detection of 5-Hydroxytryptamine Release in the Rat Brain. *Anal. Chem.* **2009**, *81*, 9462–9471.
15. Takmakov, P.; Zachek, M. K.; Keithley, R. B.; Bucher, E. S.; McCarty, G. S.; Wightman, R. M. Characterization of Local pH Changes in Brain Using Fast-Scan Cyclic Voltammetry with Carbon Microelectrodes. *Anal. Chem.* **2010**, *82*, 9892–9900.
16. Park, J.; Takmakov, P.; Wightman, R. M. *In vivo* Comparison of Norepinephrine and Dopamine Release in Rat Brain by Simultaneous Measurements with Fast-Scan Cyclic Voltammetry. *J. Neurochem.* **2011**, *119*, 932–944.
17. Herr, N. R.; Park, J.; McElligott, Z. A.; Belle, A. M.; Carelli, R. M.; Wightman, R. M. *In vivo* Voltammetry Monitoring of Electrically Evoked Extracellular Norepinephrine in Subregions of the Bed Nucleus of the Stria Terminalis. *J. Neurophysiol.* **2012**, *107*, 1731–1737.
18. Jaquins-Gerstl, A.; Michael, A. C. Comparison of the Brain Penetration Injury Associated with Microdialysis and Voltammetry. *J. Neurosci. Methods* **2009**, *183*, 127–135.
19. Wightman, R. M.; Wipf, D. O. Voltammetry at Ultramicroelectrodes. *Electroanal. Chem.* **1989**, *15*, 267–353.
20. Takmakov, P.; Zachek, M. K.; Keithley, R. B.; Walsh, P. L.; Donley, C.; McCarty, G. S.; Wightman, R. M. Carbon Microelectrodes with a Renewable Surface. *Anal. Chem.* **2010**, *82*, 2020–2028.

21. Perry, M.; Li, Q.; Kennedy, R. T. Review of Recent Advances in Analytical Techniques for the Determination of Neurotransmitters. *Anal. Chim. Acta* **2009**, *653*, 1–22.
22. Robinson, D. L.; Hermans, A.; Seipel, A. T.; Wightman, R. M. Monitoring Rapid Chemical Communication in the Brain. *Chem. Rev.* **2008**, *108*, 2554–84.
23. Dayton, M. A.; Wightman, R. M. Carbon-Fiber Microelectrodes as Invivo Voltammetric Probes of Endogenous Chemical Transmitter Concentration. *Clin. Res.* **1980**, *28*, A798–A798.
24. Dayton, M. A.; Brown, J. C.; Stutts, K. J.; Wightman, R. M. Faradaic Electrochemistry at Micro-Voltammetric Electrodes. *Anal. Chem.* **1980**, *52*, 946–950.
25. Armstrongjames, M.; Millar, J. Carbon-Fiber Micro-Electrodes. *J. Neurosci. Methods* **1979**, *1*, 279–287.
26. Bond, A. M.; Fleischmann, M.; Robinson, J. Electrochemistry in Organic-Solvents without Supporting Electrolyte Using Platinum Microelectrodes. *J. Electroanal. Chem.* **1984**, *168*, 299–312.
27. Kittlesen, G. P.; White, H. S.; Wrighton, M. S. Chemical Derivatization of Microelectrode Arrays by Oxidation of Pyrrole and N-Methylpyrrole−Fabrication of Molecule-Based Electronic Devices. *J. Am. Chem. Soc.* **1984**, *106*, 7389–7396.
28. Gerhardt, G. A.; Oke, A. F.; Nagy, G.; Moghaddam, B.; Adams, R. N. Nafion-Coated Electrodes with High Selectivity for CNS Electrochemistry. *Brain Res.* **1984**, *290*, 390–395.
29. Brazell, M. P.; Kasser, R. J.; Renner, K. J.; Feng, J.; Moghaddam, B.; Adams, R. N. Electrocoating Carbon-Fiber Microelectrodes with Nafion Improves Selectivity for Electroactive Neurotransmitters. *J. Neurosci. Methods* **1987**, *22*, 167–172.
30. Whiteley, L. D.; Martin, C. R. Fresh Look at Transport in Perfluorosulfonate Ionomers - Ultramicroelectrode Investigations of Nafion and the Dow Ionomers. *J. Phys. Chem.* **1989**, *93*, 4650–4658.
31. Singh, Y. S.; Sawarynski, L. E.; Dabiri, P. D.; Choi, W. R.; Andrews, A. M. Head-to-Head Comparisons of Carbon Fiber Microelectrode Coatings for Sensitive and Selective Neurotransmitter Detection by Voltammetry. *Anal. Chem.* **2011**, *83*, 6658–6666.
32. Engstrom, R. C. Electrochemical Pretreatment of Glassy-Carbon Electrodes. *Anal. Chem.* **1982**, *54*, 2310–2314.
33. Gonon, F. G.; Fombarlet, C. M.; Buda, M. J.; Pujol, J. F. Electrochemical Treatment of Pyrolytic Carbon-Fiber Electrodes. *Anal. Chem.* **1981**, *53*, 1386–1389.
34. Bath, B. D.; Michael, D. J.; Trafton, B. J.; Joseph, J. D.; Runnels, P. L.; Wightman, R. M. Subsecond Adsorption and Desorption of Dopamine at Carbon-Fiber Microelectrodes. *Anal. Chem.* **2000**, *72*, 5994–6002.
35. Xiao, N.; Venton, B. J. Rapid, Sensitive Detection of Neurotransmitters at Microelectrodes Modified with Self-Assembled SWCNT Forests. *Anal. Chem.* **2012**, *84*, 7816–7822.
36. Qing, W. X.; Liu, X. H.; Lu, H. M.; Liang, J.; Liu, K. Z. Ensemble of Carbon Fiber Ultra-Microelectrodes Modified with Nanotubes, and Its Application to the Determination of Dopamine. *Microchim. Acta* **2008**, *160*, 227–231.
37. Zhang, X. F.; Li, Q. W.; Tu, Y.; Li, Y. A.; Coulter, J. Y.; Zheng, L. X.; Zhao, Y. H.; Jia, Q. X.; Peterson, D. E.; Zhu, Y. T. Strong Carbon-Nanotube Fibers Spun from Long Carbon-Nanotube Arrays. *Small* **2007**, *3*, 244–248.
38. Zheng, L. X.; Zhang, X. F.; Li, Q. W.; Chikkannanavar, S. B.; Li, Y.; Zhao, Y. H.; Liao, X. Z.; Jia, Q. X.; Doorn, S. K.; Peterson, D. E.; *et al.* Carbon-Nanotube Cotton for Large-Scale Fibers. *Adv. Mater.* **2007**, *19*, 2567–2570.
39. Zhang, X. F.; Li, Q. W.; Holesinger, T. G.; Arendt, P. N.; Huang, J. Y.; Kirven, P. D.; Clapp, T. G.; DePaula, R. F.; Liao, X. Z.; Zhao, Y. H.; *et al.* Ultrastrong, Stiff, and Lightweight Carbon-Nanotube Fibers. *Adv. Mater.* **2007**, *19*, 4198–4201.
40. Mirfakhrai, T.; Oh, J.; Kozlov, M. E.; Fang, S. L.; Zhang, M.; Baughman, R. H.; Madden, J. D. W. Mechanoelectrical Force Sensors Using Twisted Yarns of Carbon Nanotubes. *IEEE/ASME Trans. Mechatron.* **2011**, *16*, 90–97.
41. Wang, J.; Deo, R. P.; Poulin, P.; Mangey, M. Carbon Nanotube Fiber Microelectrodes. *J. Am. Chem. Soc.* **2003**, *125*, 14706–14707.
42. Zhu, Z. G.; Garcia-Gancedo, L.; Flewitt, A. J.; Moussy, F.; Li, Y. L.; Milne, W. I. Design of Carbon Nanotube Fiber Microelectrode for Glucose Biosensing. *J. Chem. Technol. Biotechnol.* **2012**, *87*, 256–262.
43. Zhu, Z. G.; Song, W. H.; Burugapalli, K.; Moussy, F.; Li, Y. L.; Zhong, X. H. Nano-Yarn Carbon Nanotube Fiber Based Enzymatic Glucose Biosensor. *Nanotechnology* **2010**, *21*, 1–10.
44. Viry, L.; Derre, A.; Poulin, P.; Kuhn, A. Discrimination of Dopamine and Ascorbic Acid Using Carbon Nanotube Fiber Microelectrodes. *Phys. Chem. Chem. Phys.* **2010**, *12*, 9993–9995.
45. Harreither, W.; Trouillon, R.; Poulin, P.; Neri, W.; Ewing, A. G.; Safina, G. Carbon Nanotube Fiber Microelectrodes Show a Higher Resistance to Dopamine Fouling. *Anal. Chem.* **2013**, *85*, 7447–7453.
46. Koehne, J. E.; Marsh, M.; Boakye, A.; Douglas, B.; Kim, I. Y.; Chang, S. Y.; Jang, D. P.; Bennet, K. E.; Kimble, C.; Andrews, R.; *et al.* Carbon Nanofiber Electrode Array for Electrochemical Detection of Dopamine Using Fast Scan Cyclic Voltammetry. *Analyst* **2011**, *136*, 1802–1805.
47. Jiang, C. Q.; Li, L. M.; Hao, H. W. Carbon Nanotube Yarns for Deep Brain Stimulation Electrode. *IEEE Trans. Neural Syst. Rehabil. Eng.* **2011**, *19*, 612–616.
48. Adams, R. N. Probing Brain Chemistry with Electroanalytical Techniques. *Anal. Chem.* **1976**, *48*, 1126A–1138A.
49. Wightman, R. M.; May, L. J.; Michael, A. C. Detection of Dopamine Dynamics in the Brain. *Anal. Chem.* **1988**, *60*, 769A–779A.
50. Roberts, J. G.; Lugo-Morales, L. Z.; Loziuk, P. L.; Sombers, L. A. Real-Time Chemical Measurements of Dopamine Release in the Brain. *Methods Mol. Biol.* **2013**, *964*, 275–294.
51. Maloy, J. T. Digital Simulation of Electrochemical Problems. In *Laboratory Techniques in Electroanalytical Chemistry*, 2nd Edition ed.; Kissinger, P. T.; Heinemann, W. R., Eds. Marcel Dekker, Inc.: New York, 1996.
52. Feldberg, S. W. Digital Simulation: A General Method for Solving Electrochenical Diffusion-Kinetic Problems. In *Electroanalytical Chemistry: A Series of Advances*, Bard, A. J., Ed. Marcel Dekker: New York, 1969, Vol. 3.
53. Bard, A. J.; Faulkner, L. R. *Electrochemical Methods: Fundamentals and Applications*; Wiley: New York, 2000.
54. Jacobs, C. B.; Vickrey, T. L.; Venton, B. J. Functional Groups Modulate the Sensitivity and Electron Transfer Kinetics of Neurochemicals at Carbon Nanotube Modified Microelectrodes. *Analyst* **2011**, *136*, 3557–3565.
55. Hocevar, S. B.; Wang, J.; Deo, R. P.; Musameh, M.; Ogorevc, B. Carbon Nanotube Modified Microelectrode for Enhanced Voltammetric Detection of Dopamine in the Presence of Ascorbate. *Electroanalysis* **2005**, *17*, 417–422.
56. Henstridge, M. C.; Dickinson, E. J. F.; Aslanoglu, M.; Batchelor-McAuley, C.; Compton, R. G. Voltammetric Selectivity Conferred by the Modification of Electrodes Using Conductive Porous Layers or Films: The Oxidation of Dopamine on Glassy Carbon Electrodes Modified with Multiwalled Carbon Nanotubes. *Sens. Actuators, B* **2010**, *145*, 417–427.
57. Zachek, M. K.; Hermans, A.; Wightman, R. M.; McCarty, G. S. Electrochemical Dopamine Detection: Comparing Gold and Carbon Fiber Microelectrodes Using Background Subtracted Fast Scan Cyclic Voltammetry. *J. Electroanal. Chem.* **2008**, *614*, 113–120.
58. Kissinger, P. T.; Heineman, W. R. Laboratory Techniques in Electroanalytical Chemistry, 2nd ed.; Marcel Dekker Inc.: New York, 1984.
59. Spanos, M.; Gras-Najjar, J.; Letchworth, J. M.; Sanford, A. L.; Toups, J. V.; Sombers, L. A. Quantitation of Hydrogen Peroxide Fluctuations and Their Modulation of Dopamine Dynamics in the Rat Dorsal Striatum Using Fast-Scan Cyclic Voltammetry. *ACS Chem. Neurosci.* **2013**, *4*, 782–789.
60. Pihel, K.; Hsieh, S.; Jorgenson, J. W.; Wightman, R. M. Electrochemical Detection of Histamine and 5-Hydroxytryptamine at Isolated Mast Cells. *Anal. Chem.* **1995**, *67*, 4514–4521.

61. Hashemi, P.; Dankoski, E. C.; Wood, K. M.; Ambrose, R. E.; Wightman, R. M. *In vivo* Electrochemical Evidence for Simultaneous 5-HT and Histamine Release in the Rat Substantia Nigra Pars Reticulata Following Medial Forebrain Bundle Stimulation. *J. Neurochem.* **2011**, *118*, 749–759.
62. Chang, S. Y.; Jay, T.; Munoz, J.; Kim, I.; Lee, K. H. Wireless Fast-Scan Cyclic Voltammetry Measurement of Histamine Using WINCS—A Proof-of-Principle Study. *Analyst* **2012**, *137*, 2158–2165.
63. Banks, C. E.; Compton, R. G. Exploring the Electrocatalytic Sites of Carbon Nanotubes for NADH Detection: An Edge Plane Pyrolytic Graphite Electrode Study. *Analyst* **2005**, *130*, 1232–1239.
64. Heien, M.; Phillips, P. E. M.; Stuber, G. D.; Seipel, A. T.; Wightman, R. M. Overoxidation of Carbon-Fiber Microelectrodes Enhances Dopamine Adsorption and Increases Sensitivity. *Analyst* **2003**, *128*, 1413–1419.
65. Michael, D.; Travis, E. R.; Wightman, R. M. Color Images for Fast-Scan Cv. *Anal. Chem.* **1998**, *70*, 586A–592A.
66. Inoue, Y.; Kakihata, K.; Hirono, Y.; Horie, T.; Ishida, A.; Mimura, H. One-Step Grown Aligned Bulk Carbon Nanotubes by Chloride Mediated Chemical Vapor Deposition. *Appl. Phys. Lett.* **2008**, 92.